AIR QUALITY IN AIRPORT APPROACHES:
IMPACT OF EMISSIONS ENTRAINED BY VORTICES IN AIRCRAFT WAKES

Angus Graham and David Raper, Manchester Metropolitan

October 2003

ABSTRACT

Exhaust from aeroplanes is entrained within a pair of wingtip vortices trailing in their wake. An aeroplane exerts a downward force on the air, and so the wake must descend, as mediated through the action of the vortices on one another. Exhaust pollutants may thus be conveyed to the ground close to airports far more effectively than through ambient atmospheric dispersion alone, as has hitherto been assumed occurs within air-quality models. A kinematic model of vortex-mediated pollutant transport has therefore been developed, harnessing results from dynamical models in the literature to estimate the size of the neglected term in ground-level concentrations.

Model runs show that in (10 m) winds of 2-4 m s^{-1}, nitrogen oxides (NO_x) in the vortex wakes of narrow-body turbofan aeroplanes may contribute 2 μg m^{-3} or more to mean diurnal ground-level concentrations, up to 2 km downwind of a busy runway (Manchester Airport, R1). A mean of 29 μg m^{-3} NO_x was recorded near the airport in 2000.

Introduction

Development of infrastructure and the urban environment must be astutely managed if it is not to jeopardise air quality. Some of the largest municipal developments occur at airports, at the urban fringe. Assessment of the impact of a major airport development on air quality as well as noise levels is therefore mandatory (e.g. as in the cases of Manchester Airport 2nd Runway and T5 Heathrow). Airports must accommodate a forecast 5-7% mean annual increase in air traffic movements ('The Future of Aviation', DTLR), but there is only limited scope for reducing emissions from jet engines. Impacts are greatest locally, on people working there or living nearby in outlying suburbs, and on any areas of uncommon or protected ecology. Nitrogen oxides (NO_x) and particulates, most notably the PM_{10} group (particles smaller then 10 μm), reside along with carbon monoxide in the exhaust streams of aircraft, road and service vehicles and power and heating plants.

Airport air-quality models show little sign of converging to monitoring data (BAA, 1996; Rogers *et al*, 2002). The research described herein focuses on a dispersive process in the vicinity of airports not currently represented in the models, which may significantly and negatively impact upon ground-level concentrations of pollutants in the airport environs. Models might therefore be brought a step closer to reality by incorporating it, and the principal aim of the research is correspondingly to quantify the neglected term. The research should help inform future monitoring programmes and measurement campaigns in the vicinity of airports, and allow the relative contributions of sources there to be identified more accurately.

Emissions from aircraft are both substantial and - during the ground run, takeoff and landing - unavoidable. A jet aeroplane of several hundred passengers capacity (e.g. 757, 767) combusts fuel in flight at a rate some three orders of magnitude greater than does a car on a motorway (ICAO, 1993). Emissions are not transmitted to the ground simply through a weak process of atmospheric dispersion, however, as even the best models assume to date. To generate lift, an aeroplane must exert a downward force on the air through which it flies, and so exhausts tend to descend toward the ground within the aircraft's wake. The wake descends in an essentially inviscid and thus long-lived manner, moreover, through the action of a pair of trailing counterrotating vortices on one another, as shown in Fig. 1. The vortices derive from the circulation yielding the lift over the wings. Observations have demonstrated their rollup and entrainment of emissions in the near wake and transport of emissions thereafter (Sussmann, 1999). Their presence at ground level in the vicinity of airports is well-established, as it is the need to wait for their decay, for the safety of the following aeroplane, that caps takeoff and arrival rates at busy periods.

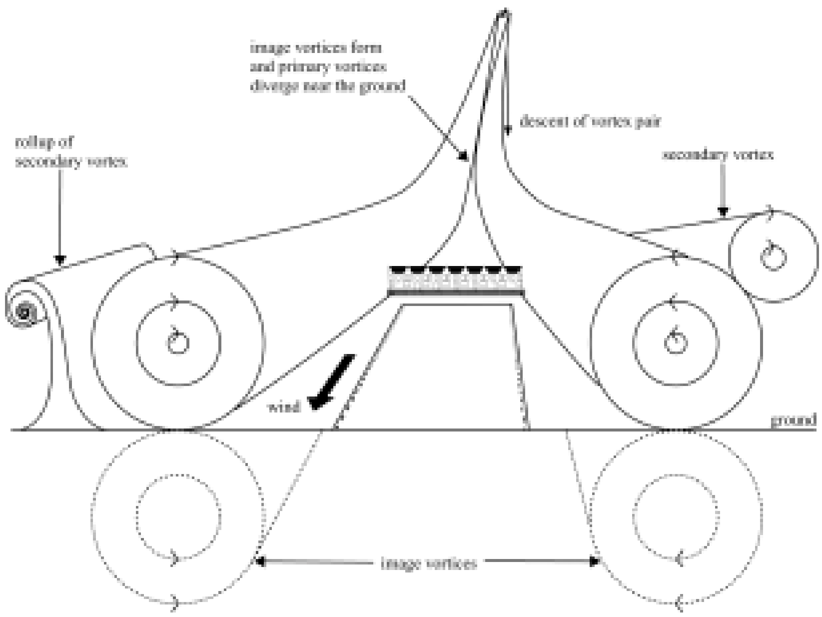

FIG. 1. Sketch of vortical flows in the wake of an aeroplane shortly after takeoff.

Methodology

The entrainment and dispersion of emissions in the vortex pair trailing behind an aeroplane may be reproduced through a use of computational fluid dynamics (CFD) within models (Gerz and Holzäpfel, 1999). As will be seen, however, such models cannot as yet adequately capture the interaction of the pair with the ground, and are moreover too computationally expensive to be used to calculate mean concentrations, as averaging over many aircraft and a wide range of meteorological conditions. A simplified, kinematic computer model has therefore been developed instead, in which the transport of emissions within vortices is *presupposed*. The model builds on experimental studies and dynamical models in the literature, however, its free parameters being set using their findings.

Predictions are made of the impact of the vortex-mediated transport, and dispersion of associated remnant emission plumes once vortices expire, on ground-level concentrations of NO_x (particulates are also of concern to regulators of emissions, but accurate emission indices of these are not available). Over the short time scales pertinent to dispersion in an airport environs, any photochemically-mediated loss of NO_x to organic nitrates or nitric acid is insignificant, and may be ignored. Concentrations are calculated by subdividing the wake longitudinally into elements. The dispersion of each element is evaluated, and concentrations are calculated simply from its diffusion scales, without any modelling of subelemental variations in concentration laterally along the ground (instantaneous distributions cannot be assumed to conform to Gaussian statistics). Any dynamical interaction between vortices from different aircraft or dispersion by vortices of remnant plumes surviving from earlier aircraft is assumed not to impact on mean concentrations significantly and ignored, although plumes themselves are free to overlap.

A schematic of the model domain adopted is shown in Fig. 2. Aircraft are assumed to takeoff and land into the wind (airports may in reality take other factors into account when selecting the operational direction in low winds). Geometries adopted reflect those of Manchester Airport (R1). The runway is 3 km long, and oriented along 60-240º. An ILS landing system is employed at the airport, with incoming aircraft being guided in along the axis of a radar beam inclined upward at 3º.

The model may be broken down into five components, outlined as below.

a) FLIGHT DYNAMICS

Aeroplanes may for present purposes be taken to lift off a certain distance upwind of the downwind runway end, depending on their thrust and lift characteristics and weight, and to touch down a sixth of the runway length upwind of the downwind end. The aeroplane's course elevation is taken as constant throughout takeoff as well as landing. The transitional trajectory regimes immediately after lift-off and in the landing flare before touchdown are not represented, therefore, and there is no manoeuvring of the aeroplane later in takeoff in the section of the flight path of interest. Flight-path restrictions permit manoeuvring only when the aeroplane has climbed to an altitude of at least 300 m, a height which vortices rarely survive long enough to descend through. During takeoff, flaps and slats are assumed maintained at initial settings and the undercarriage to be retracted at an altitude of 60 m. In the landing approach, flaps and slats are assumed fully extended (for maximum drag), and the undercarriage to be down throughout.

The thrust from the engines may be taken to act along the flight path. It falls as aircraft speed rises, applying as it does net of internal engine drag (although this is partly offset at significant Mach fractions in turbofans by a compression of the inlet stream, so that the compressor draws less power). The drag on the aeroplane is assumed to satisfy a drag-polar law, drag coefficient increasing linearly with the square of lift coefficient (the relation stems from the offset of aeroplane attitude to its course). The maximum course elevation employable during takeoff is that such that thrust, drag and weight forces balance, so there is no power available to work against inertia and induce an acceleration. The course elevation actually adopted is set as a prescribed fraction of the maximum, currently equal to 0.85. In the landing approach, forces are assumed in balance down to an altitude of 60 m, after which no further power is drawn from the engines and the aeroplane decelerates (see Mair and Birdsall, 1992). The descent takes place throughout at a declination of 3º, as described earlier.

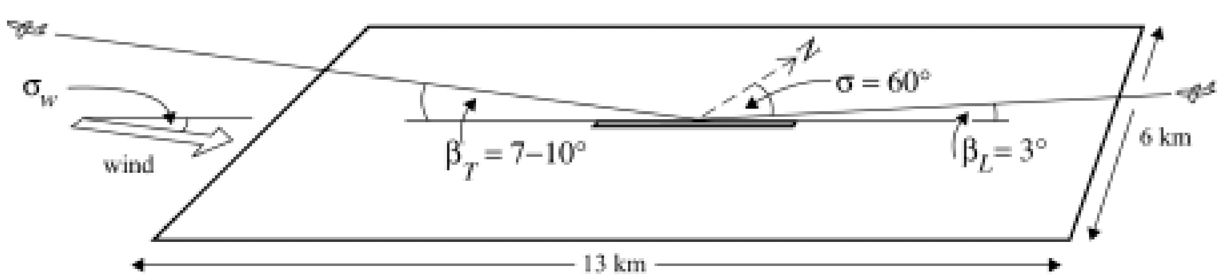

FIG. 2. Sketch of the model domain. The runway lies along an angle, σ, right of north and an angle, σ_W, right of the direction from which surface winds blow. Aircraft approach it at an elevation, β_L, and take off at an elevation, β_T.

b) VORTEX MATURATION

The lift on an aerofoil arises through the circulation about it. This circulation, once generated, is conserved, and must therefore be lost to the wake. Well away from the ground, the wake of a wing pair contains a pair of streamwise counterrotating vortices deriving from the bound circulation, as roll up within a few wingspans downstream (see http://www.cerfacs.fr/~wakenet). The vortex pair moves off normally to the flight path through mutual induction (see Fig. 1). Additional persistent streamwise vortices may arise in the wake of more complex aerodynamic forms, as forced at fuselage walls or from a differential setting of inboard and outboard flaps, but measurements and models generally support the existence of a single pair (Spalart, 1998).

Emissions are entrained very efficiently as vortices roll up. Above the aircraft contrails often evident at high altitudes to the casual observer, visible as a result of expelled water vapour condensing, a detached, secondary wake remaining at the level of the aircraft can frequently be discerned, but this probably results from ice formation in supersaturated conditions (Sussman, 1999; Sussman and Gierens, 1999). Both the buoyancy of exhausts and the location of the engine on the airframe affect the initial distribution of emissions, but simulations do not reveal any clear trend of emissions ultimately to evade capture by the vortices (Lewellen and Lewellen, 1996; Gerz and Ehret, 1997). Initial losses are thus assumed for purposes here to be negligible.

Exhaust buoyancy may affect the dispersion of emissions generated during the ground run (see http://www.aee.faa.gov/emissions/EDMS/Lidar-2002.pdf). It is, however, unlikely to impact on the dispersion higher up, once vortices have rolled up. Exhausts are subject to a much greater dilution away from the ground, as aircraft speeds are greater, and wakes are free to grow by entrainment from below as well as above.

If the aeroplane is sufficiently near to the ground, the rollup of the vortex pair will be impeded (through a separation of secondary vorticity from the ground and incorporation of this into the wake in the upward flow at lateral wake margins). This effect is dealt with simply in the model, by taking the pair to be entirely suppressed if the aeroplane altitude is less than half a wingspan, but otherwise to be unaffected.

c) FREE-VORTEX DYNAMICS

Mature vortices in the far wake of aircraft decay only slowly through turbulent dissipation (Spalart, 1998). The characteristic lifetime of a vortex pair well away from the ground is instead in the main held to result from a growth of Crow instability (Crow, 1970; Crow and Bate, 1976; Han *et al*, 2000; Sarpkaya, 2000). In this, vortices develop symmetric undulations in perpendicular planes, as sketched in Fig. 3, until cores merge and annihilate at the line of symmetry. Eddies in the ambient turbulence field of scale somewhat larger than the mean spacing of cores force the growth.

The descent of the vortices and development of the instability need not, it is contended, be considered during periods of moderately or strongly stable stratification. Any vortex-mediated transfer of emissions to the ground in these conditions is unlikely to contribute significantly to local mean concentrations, for the following two reasons. Firstly, as the vortices descend, they become hotter than their surroundings, and may rupture when buoyancy forces exceed centripetal forces. Numerical studies show a shedding of vortex contents to a buoyant secondary wake in stable stratification (Schilling *et al*, 1996; Gerz *et al*, 1998; Holzäpfel and Gerz, 1999). Secondly, where vortices persist to encounter the ground, they start to pair off with their images and move apart (see *d* below). As the downward forcing abates, vortex buoyancy is no longer counteracted, and a trend for vortices to return upward may be anticipated.

In convective conditions, the potential-temperature gradient in the atmospheric mixed layer is marked only near the surface. With vortex descent in the surface layer generally retarded by the presence of the ground (see *d* below), convection is consequently taken to impact on vortex dynamics only indirectly, through its influence on turbulence levels. Crow and Bate (1976) parameterise the turbulent forcing of their instability by taking the mediating eddies to lie in the inertial subrange. With interest here confined to the lower boundary layer, this assumption will not generally be valid, but as the turbulent-dissipation rate can in any case only be predicted to within an order of magnitude from standard meteorological measurements, their parameterisation is retained.

Vortices are advected by the mean wind, which must therefore also be parameterised. The wind-speed profile in the convective surface layer may be calculated from standard meteorological measurements (Stull, 1988). Above this, winds are assumed subject to a clockwise rotation (a northern-hemisphere location thus being presupposed). Cartesian components, in a frame oriented with the surface wind, are extrapolated linearly from the top of the surface layer to the height of convective equilibration.

The vortex induction velocity will generally be tilted a little from the vertical, as a result of the elevation of the flight path, and any vortex stretching or shrinking in the mean shear or shear-induced tilting of the pair. These effects are neglected. A shear-induced reorienting of vortices' axes in the azimuth is, however, allowed for, as cross-winds influence the interaction with ground (see *d* below).

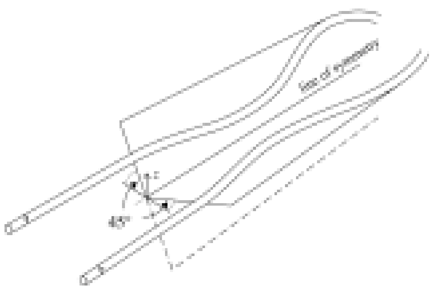

FIG. 3. Sketch of the onset of Crow instability in the vortex pair in the wake of an aeroplane. The dashed lines show the extrapolation of the left-hand vortex plane below the right-hand vortex (see *d* below).

d) GROUND INTERACTION

As the ground is impermeable on all but the microscale, image vortices must arise (Fig. 1). The advective velocities of vortices due to images become significant once vortices are within about two wingspans of the ground, and vortices start to move apart and pair off with their images. The flow along the ground forced by the vortex and image system also forces the growth of a shear layer there. While this is confined at the ground, vortex dynamics remain essentially inviscid. After a critical time, however, the inviscid approximation breaks down, the shear layer separates from the ground and secondary-vortex-rollup occurs (Doligalski *et al*, 1994). The secondary draws the primary away from the ground with it, and the two execute a joint oscillatory motion (primaries are then too widely spaced for this to impact much on the motion of the other).

A wind, if present and not aligned with primaries, may bolster the vortex-induced flow at the ground, speeding separation up, or oppose it, slowing separation down. If, in the latter case, the wind is strong enough, an upward displacement of mean streamlines upwind of the vortex can be arrested downwind, as can be seen from Fig. 4, and the viscous response is muted (see Doligalski *et al*, 1994). Two-dimensional numerical models of vortex-pair descent support an asymmetric viscous response in the presence of a crosswind, with complete suppression of a secondary if crosswinds are high (Zheng and Ash, 1996; Corjon and Poinsot, 1997).

Three-dimensional effects are likely important, particularly in light of the inclination of vortices' axes stemming from the inclined flight path. Unfortunately, numerical models with ground-effect cannot capture these effects adequately at present, and their modelling here is thus necessarily speculative.

A Crow instability may develop between a primary vortex and its image. As the line of symmetry is the same as holds in the case of primaries far off ground (see Fig. 3), perturbations excited high up may continue to grow unchecked as primaries approach the ground, and the instability may run to completion before viscous separation occurs. Where vortices originate lower down, a secondary vortex may be presumed to rollup and arrest the Crow instability. A complex dynamics will then take shape, with primary and secondary vortices oscillating broadly in phase with one another while being advected by the wind and to some degree by their images, and with further secondary vortices perhaps being generated. Separation of secondary vorticity will occur at different times along primaries' axes according to the initial height of vortex sections and their subsequent perturbation by the Crow instability while descending. Three-dimensional interactions will likely cause secondaries to wrap around primaries and ultimately merge with them.

The oscillations occurring after separation of secondary vorticity need not themselves be represented. Primaries are instead treated as if advected by wind and image at a mean height and velocity deducible from 2-D numerical studies (Zheng and Ash, 1996; Corjon and Poinsot, 1997). Such studies cannot shed light on the effective lifetime of primaries following separation, however, and uncertainty as to the value of this is probably that which is limiting in the model. As currently specified, lifetimes may reach up to about ten times the time primaries take to descend through a height equal to their spacing, well away from ground.

e) PLUME DIFFUSION

It is hypothesised that vortices break up through a merging either with images or with secondary vortices (see *d* above). After a rapid turbulent dissipation of vortex energies takes place (a complex process that is not represented), entrained emissions will begin to diffuse in the ambient turbulence as a remnant plume superseding the vortex.

Where a Crow instability of primary and image goes to completion and cores merge, emissions arise at the ground at the onset of the diffusion. Characteristic horizontal and vertical scales of a plume cross section at this time are ascribed allowing for a likely flattening of vortices. Where breakup occurs off ground, emissions are manifest permanently at the ground only after a period of diffusion through the underlying air at breakup. In both cases, plume scales are assumed to evolve linearly over diffusion time, following an identification from the literature of characteristic diffusion velocities in the atmospheric surface layer (Gifford, 1961; Irwin, 1979; Webb, 1982; Hogstrom, 1988). Where plumes are checked at the ground, a zone of enhanced near-ground concentrations develops. This is taken into account when calculating the height of plume centroids (as vertical diffusion velocities depend on centroid height). Relations are, for simplicity, applied even when centroids rise above the surface layer, as concentrations are not then significant.

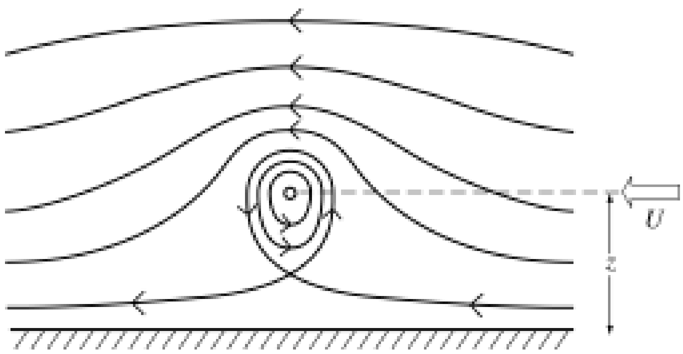

FIG. 4. Sketch of streamlines in an inviscid 2-D flow in a fixed frame of reference, in which a line vortex of strength, Γ, arises a distance, *z*, from a boundary in a uniform flow, *U*, satisfying $U>\Gamma/(\pi z)$.

aeroplane							engine				
		C_{L1}		$k_{D1} \times 10^{-2}$				$q_e/Q_e \times 10^{-3}$			
S/B^2	max $\Delta W/W_0$	a) takeoff	b) landing	a) takeoff	b) landing	$k_{D2} \times 10^{-2}$	max F_e/W_0	a) idling	b) max Q_e	k_{F1}	k_{F2}
0.126	0.77	2.2	2.7	4	9	4.3	0.28	2.1	17.7	0.83	0.47

TABLE 1. Dimensionless flight and performance parameters of the 737-300, as fitted with two CFM56-3B-1 turbofan engines. The aeroplane has a wingspan, B, equal to 28.9 m, and an empty weight, W_0, corresponding to a mass of 31.9 tonnes. Fuel consumption per engine, Q_e, is of maximum, 0.95 kg s^{-1}. Engines idle at 7% this. Wing plan-form area is denoted S, and aeroplane load, ΔW. Maximum lift coefficient is denoted C_{L1}. The drag coefficient is assumed to scale linearly with square lift coefficient, the constant of linearity being denoted k_{D1}, and the coefficient of linearity, k_{D2}. Values adopted for k_{D1} and k_{D2} follow from sparse data in the open literature (Torenbeek, 1982; Mair and Birdsall, 1992). Flaps and slats are assumed partly extended for takeoff and fully extended for landing. Values for k_{D1} apply, furthermore, with the undercarriage retracted. Static thrust per engine is denoted F_e, and NO_x source strength per engine, q_e. Dynamic thrust per engine is assumed to depend quadratically on airspeed. With fractional changes on static values cast as a function of airspeed normalised on sound speed, the linear term is of coefficient, $-k_{F1}$, and the quadratic term of coefficient, k_{F2}. Values of these follow from the literature as above. Emissions data derive from the ICAO (http://www.qinetiq.com/aircraft.html).

Results

Preliminary results are presented. A single aircraft, the 737-300, is considered, but mean concentrations are calculated on taking this as representative of narrow-body aircraft in general. Parameters of its flight are given in Table 1. Three reference takeoff loads are considered, equal to 40%, 60% and 80% maximum. Fuel consumption of the 737-300 at takeoff typically ranges through 86-90% maximum over these loads (BAA, unpublished data). Mean concentrations are calculated by taking the lightest load as representative of the lightest sixth of takeoffs and the heaviest load as representative of the heaviest half. The landing load is taken as 40% maximum.

Four times are simulated during a sunny, midsummer weekday. These constitute 0800, 1300, 1800 and 2100 hrs. It is assumed flights take place over 0700-2300 hrs, two-thirds of them involving narrow-body aircraft. Between 0700-0900 and 1700-1900, the runway is taken to operate at a capacity of 45 aircraft movements per hour (Manchester Airport, R1), and to operate at half-capacity otherwise. A wind (at 10 m) of 2-4 m s^{-1} blows from the southwest, 20º anticlockwise of the runway, until after the evening peak in operations, when it swings clockwise through 30º.

The model computes the evolving ground-level concentration field resulting from individual flights. An illustrative time series is shown in Fig. 5. Here, vortices descending from initial heights of up to about four times the wingspan survive to prompt a significant ground action. The plots capture the ground-level signature of two plumes, drifting downwind and spreading in the horizontal and vertical, so that concentrations fall. Crosswinds are too small to induce significant asymmetries between the plumes, through a staggered viscous response at the ground (see Methodology *d* above). Plume axes are offset slightly to the flight path in the horizontal, as a result of a reorientation of vortices by the mean shear as they descend (see Methodology *c* above).

The plumes are initially discontinuous (Fig. 5a). The left-hand parts stem from times when the aircraft was at relatively low altitude, so vortices force viscous separation from the ground before a Crow instability with images can go to completion (see Methodology *d* above). The associated diffusion of plumes to the ground following vortex expiration is incomplete. The right-hand parts stem from times when the aircraft was higher up, so the instability with images goes to completion before separation can occur. Plumes overlap, as vortices expire before moving far from one another under the action of their images, and are flattened as cores approach the ground.

Plumes later attain their full length at the ground (Fig. 5b). An order-of-magnitude discontinuity in concentrations can be seen about halfway along them, corresponding to a reduction in emissions when the aeroplane reached an altitude of 60 m, and engines were powered down for maximum deceleration. The discontinuity is smeared out later as a result of longitudinal dispersion processes (Fig. 5d). The plumes have also merged along their line of symmetry by this time, and concentrations thus reach a maximum here.

The concentration field as averaged over many flights, using simulations at the four selected times of day, is shown in Fig. 6. The shift in wind direction is evident (but incompletely resolved). Values reach 2 μg m^{-3} or more up to 2 km downwind of the runway. The largest values derive from late evening (the time holding in the case of Fig. 5), despite the low volume of air traffic then pertaining, indicating a strong sensitivity to conditions. Winds are lower at this time and the Monin-Obukhov length more negative. Vortices thus relay emissions to the ground from a greater height in the lower turbulence (see Methodology *c* above), and plumes are present for longer at a given point on the ground.

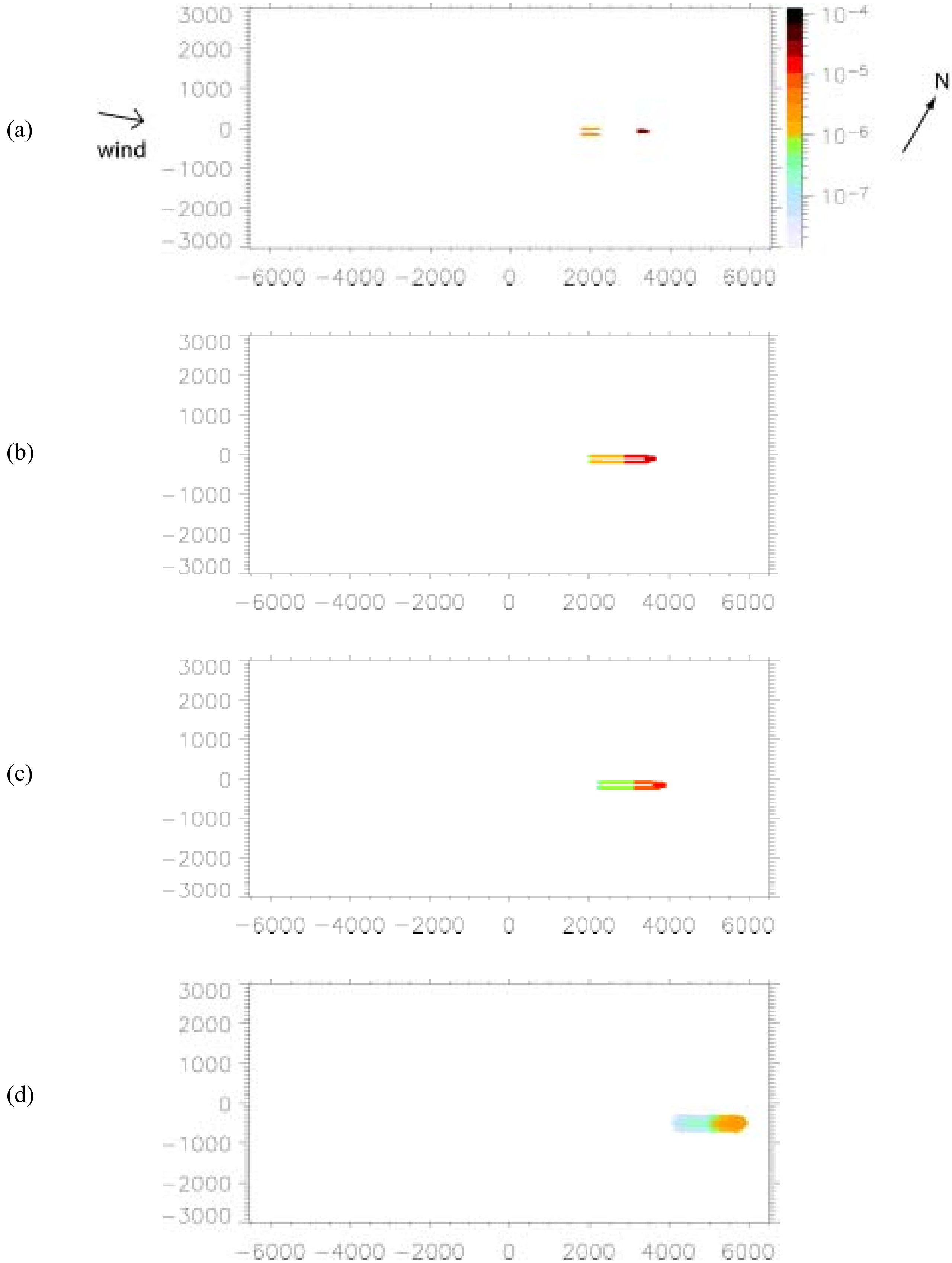

FIG. 5. Predicted ground-level NO_x concentration fields (g m^{-3}), lengths in metres, resulting from a 737 approaching a 3-km runway, centred at the origin, from the right: time after touchdown a) 199 s, b) 299 s, c) 419 s and d) 1277 s. The aeroplane is as described in Table 1. Wind at 10 m is 2.0 m s^{-1} directed as shown left, with north pointing as shown right. The approach takes place at 2100 hrs; Monin-Obukhov length is –3 km. A roughness length of 2 cm is assumed, with the surface layer extending to a height of 55 m (Stull, 1988). The wind equilibrates convectively at 400 m at a speed of 3.8 m s^{-1}, and as offset 45º clockwise of its direction at the surface. Mixing-layer height is 1600 m.

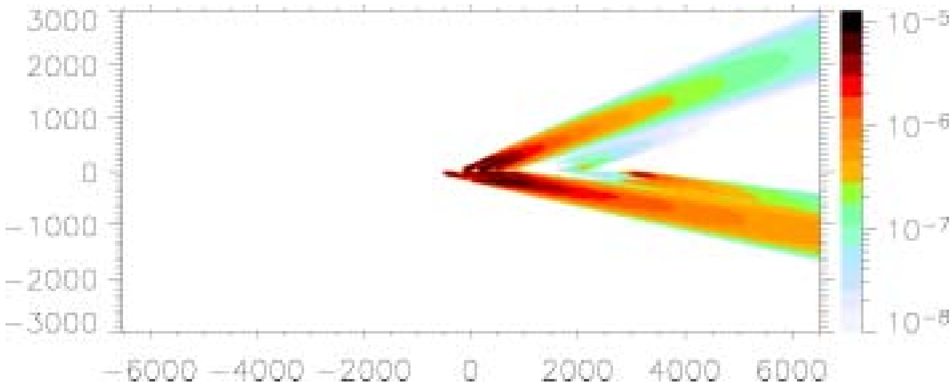

FIG. 6. Predicted ground-level NO_x concentration field as averaged over 24 hrs.

Concluding Remarks

(*i*) A novel model of the entrainment and transport of aircraft exhausts to the ground in wake vortices has been developed. A kinematic approach has been employed, as emissions transported in such a concentrated, highly intermittent manner impact on mean ground-level concentrations in a way difficult to determine using standard dispersion models or dynamical models. Results from validated dynamical models have, however, been drawn upon.

ii) Model runs show that in (10 m) winds of 2-4 m s^{-1}, nitrogen oxides (NO_x) in the vortex wakes of narrow-body turbofan aeroplanes may contribute 2 µg m^{-3} or more to mean diurnal ground-level concentrations, up to 2 km downwind of a busy runway (Manchester Airport, R1). The UK target for annual mean NO_2 is 40 µg m^{-3}. A mean of 29 µg m^{-3} NO_x was recorded in 2000 1.2 km longitudinally from the runway, in the prevailing downwind direction (prior to R2: see http://www.airquality.co.uk). The vortex-mediated term may well prove significant, therefore, once wide-body aircraft are accounted for and annual means are obtained.

REFERENCES

BAA. 1996. Air quality implications of Heathrow T5: comparisons of measured and modelled concentrations for 1993/4. BAA/811, British Airports Authority, London.
Corjon, A. and Poinsot, T. 1997. Behaviour of wake vortices near ground. *AIAA J.*, **35**, 849-855.
Crow, S. C. 1970. Stability theory for a pair of trailing vortices. *AIAA J.*, **8**, 2172-2179.
Crow, S. C. and Bate, E. R. 1976. Lifespan of trailing vortices in a turbulent atmosphere. *J. Aircraft*, **13**, 476-482.
Doligalski, T. L., Smith, C. R. and Walker, J. D. A. 1994. Vortex interactions with walls. *Annu. Rev. Fluid Mech.*, **26**, 573-616.
Gerz, T., Dürbeck, T. and Konopka, P. 1998. Transport and effective diffusion of aircraft emissions. *J. Geophys. Res.*, **103**, 25905-25913.
Gerz, T. and Ehret, T. 1997. Wingtip vortices and exhaust jets during the jet regime of aircraft wakes. *Aerosp. Sci. Technol.*, **7**, 463-474.
Gerz, T. and Holzäpfel, F. 1999. Wingtip vortices, turbulence and the distribution of emissions. *AIAA J.*, **37**, 1270-1276.
Gifford, F. A. 1961. Use of routine meteorological observations for estimating atmospheric dispersion. *Nucl. Safety*, **2**, 47-51.
Han, J., Lin, Y.-L., Schowalter, D. G., Arya, S. P. and Proctor, F. H. 2000. Large eddy simulation of aircraft wake vortices within homogeneous turbulence: Crow instability. *AIAA J.*, **38**, 292-300.
Hogstrom, U. 1988. Non-dimensional wind and temperature profiles in the atmospheric surface layer: A re-evaluation. *Bound. Layer Meteorol.*, **42**, 55-78.
Holzäpfel, F. and Gerz, T. 1999. Two-dimensional wake vortex physics in the stably stratified atmosphere. *Aerosp. Sci. Technol.*, **5**, 261-270.
ICAO. 1993. International standards and recommended practices, environmental protection. Annex 16 to the Convention on International Civil Aviation, vol. II, *Aircraft Engine Emissions*, 2nd edition, International Civil Aviation Organisation, Montreal.
Irwin, J. S. 1979. *Scheme for Estimating Dispersion Parameters as a Function of Release Height*. EPA-600/4-79-062, US Environmental Protection Agency, Washington DC.
Lewellen, D. C. and Lewellen, W. S. 1996. Large-eddy simulations of the vortex-pair breakup in aircraft wakes. *AIAA J.*, **34**, 2337-2345.
Mair, W. A. and Birdsall D. L. 1992. *Aircraft Performance*. University Press, Cambridge, 300 pp.
Rogers, H. L., Lee, D. S., Raper, D. W., Forster, P. M., Wilson, C. W. and Newton, P. J. 2002. The impacts of aviation on the atmosphere. *Aeronaut J.*, **106**, 521-546.
Sarpkaya, T. 2000. New model for vortex decay in the atmosphere. *J. Aircraft*, **37**, 53-61.
Schilling, V., Siano, S. and Etling, D. 1996. Dispersion of aircraft emissions due to wake vortices in stratified shear flows: a two-dimensional numerical study. *J. Geophys. Res.*, **101**, 20965-20974.
Spalart, P. R. 1998. Airplane trailing vortices. *Annu. Rev. Fluid Mech.*, **30**, 107-138.
Stull, R. B. 1988. *An Introduction to Boundary-Layer Meteorology*. Kluwer, Dordrecht, 666 pp.
Sussmann, R. 1999. Vertical dispersion of an aircraft wake: aerosol-lidar analysis of entrainment and detrainment in the vortex regime. *J. Geophys. Res.*, **104**, 2117-2129.
Sussmann, R. and Gierens, K. M. 1999. Lidar and numerical studies on the different evolution of vortex pair and secondary wake in young contrails. *J. Geophys. Res.*, **104**, 2131-2142.
Torenbeek, E. 1982. *Synthesis of SubsonicAirplane Design*. University Press, Delft, 598 pp.
Webb, E. K. 1982. Profile relationships in the superadiabatic surface layer. *Q. J. R. Meteorol. Soc.*, **108**, 661-688.
Zheng, Z. C. and Ash, R. L. 1996. Study of aircraft wake vortex behaviour near the ground. *AIAA J.*, **34**, 580-589.